The Dual-Function Disabled-1 PTB Domain Exhibits Site Independence in Binding Phosphoinositide and Peptide Ligands†

Peggy C. Stolt, Didem Vardar, and Stephen C. Blacklow*

Department of Pathology, Harvard Medical School and Brigham and Women's Hospital, 77 Avenue Louis Pasteur, Boston, Massachusetts 02115

Received May 5, 2004; Revised Manuscript Received June 17, 2004

ABSTRACT: While typical intracellular protein modules have only one ligand-binding site, there are rare examples of single modules that bind two different ligands at distinct binding sites. Here we present a detailed mutational and energetic analysis of one such domain, the phosphotyrosine binding (PTB) domain of Disabled-1 (Dab1), which binds to both peptide and phosphoinositide (PI) ligands simultaneously at structurally distinct binding sites. Through the techniques of isothermal titration calorimetry (ITC), analysis of Dab1 PTB domain mutants, and nuclear magnetic resonance (NMR), we have evaluated the characteristics of binding of the Dab1 PTB domain to various peptide and PI ligands. These studies reveal that the presence of saturating concentrations of one ligand has little effect on the binding constant for a second ligand at the other site. In addition, proteins with single-point mutations in the peptide-binding site retain native affinity for PI ligands, while proteins with mutations that prevent PI binding retain native affinity for peptide. NMR titrations show that the final structure of the ternary complex is the same independent of the order of addition of the two ligands. Together, these studies show that binding of peptide and PI ligands is energetically independent and noncooperative.

Functional studies of cytosolic proteins often focus on the roles of individual protein domains. Typical domains are small 50−150-amino acid modules that usually carry out specific tasks, such as binding to a partner protein. Known domain families, which fall into ∼50−60 structural classes, are found in adaptor, scaffolding, and signaling proteins as well as enzymes and transcription factors (*1*). In addition, certain domain superfamilies in which members share similar protein scaffolds but are distinguished by their ligand specificity have been identified. This categorization supports the generally held idea that one domain performs one discrete function, while further interactions are facilitated by additional domains.

For a typical domain, there usually exists a canonical binding mode, often tailored to confer biological specificity. Characteristic binding modes and motifs for many domains, like the well-characterized Src homology domains SH2[1] and SH3, have been identified through structural as well as selection studies. Typical SH2 domains bind phosphotyrosine sequences, with selectivity for phosphotyrosine resulting from electrostatic interactions with a conserved buried arginine, and specificity for flanking sequences established by ligand residues C-terminal to the phosphotyrosine (*2*, *47*). SH3 domains typically bind proline-rich motifs (*3*−*5*) via shallow binding clefts created by conserved aromatic residues, with ligands bound in a polyproline type 2 helix conformation (*6*−*8*). Though recognition of canonical motifs in the standard binding mode is the rule, there are also examples of SH2 and SH3 domains that exhibit selective recognition of noncanonical sequences as well (*9*−*11*).

Here, we focus on a member of another common class of protein domains, the phosphotyrosine binding (PTB) domain. The PTB domain is part of the pleckstrin homology (PH) domain superfold, which includes the PH, PTB, Ena/Vasp homology (EVH1), and Ran-binding domain families (*12*). These protein modules share a similar structural scaffold consisting of a β-sandwich capped by a C-terminal α-helix but exhibit distinct ligand specificities and mechanisms of binding.

The PTB domain was originally identified as a domain that bound to a phosphorylated tyrosine within an NPXpY motif (*13*−*15*). Binding typically occurs through β-strand addition of the C-terminal peptide residues, with the N-terminal NPXpY motif in a type I β-turn, and the phosphotyrosine residue in a charged pocket formed by the loops between the β-strands. Since their discovery, PTB domains have revealed an ability to interact with a much more diverse set of ligands, including nonphosphorylated NPXpY motifs (*16*) and even non-tyrosine motifs (*17*−*19*), most of which bind in a similar manner. In addition, several PTB domains have been shown to bind to phosphoinositides (PIs) as well, like their PH domain relatives (*16*, *20*−*24*).

† This work was supported by NIH Grant HL-61001 to S.C.B. S.C.B. is a Pew Scholar in the Biomedical Sciences and an Established Investigator of the American Heart Association. P.C.S. was a National Science Foundation pregraduate fellow while this work was being carried out. D.V. is an American Cancer Society postdoctoral fellow.

* To whom correspondence should be addressed. Phone: (617) 525-4413. Fax: (617) 525-4414.

[1] Abbreviations: ApoER2, apolipoprotein E receptor 2; Dab1, Disabled-1; IL-6, interleukin-6; ITC, isothermal titration calorimetry; LIF, leukemia inhibitory factor; NMR, nuclear magnetic resonance; PTB, phosphotyrosine binding; PH, pleckstrin homology; PI, phosphoinositide; PI-4,5P_2, phosphoinositide 4,5-bisphosphate; PI-3,4,5P_3, phosphoinositide 3,4,5-triphosphate; I-4,5P_2, inositol 4,5-bisphosphate; SH2, Src homology 2; SH3, Src homology 3.

10.1021/bi049092l CCC: $27.50
Published on Web 08/03/2004

Disabled-1 (Dab1) is an adaptor protein that mediates neuronal migration during development through the association of its N-terminal PTB domain with lipoprotein receptors (*25*−*27*). The Dab1 PTB domain has a strong preference for binding to NPXpY motifs with a nonphosphorylated tyrosine (*17*). Additionally, in contrast to most small protein interaction domains, which typically adhere to a "one domain−one ligand" paradigm, the Dab1 PTB domain is unusual in its capacity to bind both peptide and PI ligands simultaneously.

Crystal structures of the Dab1 PTB domain bound simultaneously to peptides from either the apolipoprotein E receptor 2 (ApoER2) or the Alzheimer's precursor protein (APP) cytoplasmic domain and the PI-4,5P_2 headgroup reveal that binding of the two ligands occurs through discrete binding sites (*28*, *29*). In the ternary complex of the Dab1 PTB domain with the ApoER2 peptide and PI-4,5P_2, the peptide ligand adopts the canonical binding mode but discriminates against phosphorylated tyrosine in the NPXpY motif via two loops that create a pocket for the tyrosyl side chain. The association is stabilized by hydrogen bonds between the backbone amides and carbonyls of the protein and peptide ligand, as well as hydrophobic interactions. The PI moiety binds in a shallow pocket on the opposite face of the PTB domain that is formed by a group of basic residues, which are located in the position equivalent to the PI binding site on many PH domains. The phosphates from PI-4,5P_2 are coordinated by five residues; all residues are within hydrogen bonding distance of either the 4-phosphate, the 5-phosphate, or both (Figure 1; *28*).

Since the Dab1 PTB domain serves as a binding module for both peptide and PI ligands, we have chosen this protein domain as a model system to examine the interdependence of two binding sites, one for peptide and one for phosphoinositide, on the same structural scaffold. Using isothermal titration calorimetry (ITC), site-directed mutagenesis, and nuclear magnetic resonance (NMR), we have evaluated the characteristics of binding of the Dab1 PTB domain to various ligands. Our binding and mutational studies establish that binding of the peptide and PI ligands is energetically independent and noncooperative.

EXPERIMENTAL PROCEDURES

Creation of Disabled-1 PTB Domain Mutants. The murine Disabled-1 PTB domain, encompassing amino acids 20−175, was introduced into the pDEST15 vector downstream of glutathione *S*-transferase (GST) as described previously (*28*). This plasmid was used as a template for PCR mutagenesis using the Quick-Change Site-Directed Mutagenesis kit (Stratagene). The following mutants of the PTB domain were created: K45A, K45Q, K45E, H81A, H81Q, K82A, K82Q, K45E/K82Q, S114Y, and F158V. Mutations were verified by dideoxy sequencing. Native and mutant proteins were purified as described previously (*28*).

Circular Dichroism. Native and mutant Dab1 PTB domains were dialyzed exhaustively into 10 mM Na_2HPO_4 buffer (pH 7.0) containing 150 mM NaCl and 0.2 mM DTT. Far-UV wavelength scans were performed on an AVIV circular dichroism spectropolarimeter in a cell with a path length of 0.1 cm. Each sample was scanned five times from 260 to 200 nm at 4 °C, in 1 nm steps, with a signal averaging time of 3 s/nm. The resulting average spectra were baseline-corrected and plotted using KaleidaGraph.

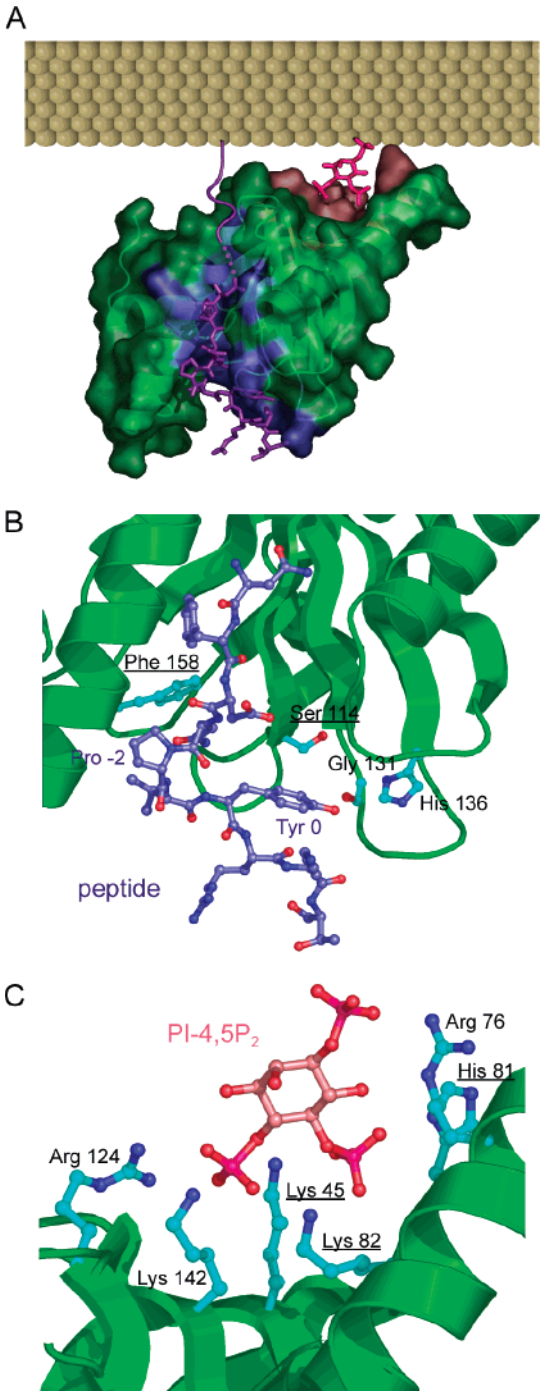

FIGURE 1: Model for the interaction among Dab1, ApoER2, and PI-4,5P_2. (A) Structure of the Dab1 PTB domain ternary complex. The Dab1 PTB domain is shown as a semitransparent molecular surface representation (green), while the ligands are shown in ball-and-stick representation. The peptide and the surface residues of the PTB domain in contact with it are lavender. PI-4,5P_2 and residues contacting it are colored salmon. The plasma membrane is highly schematized. (B) Residues involved in peptide binding. Labels of residues mutated in this work are underlined. (C) Residues involved in PIP binding. Labels of residues mutated in this work are underlined. The coordinates of the ternary complex, deposited as PDB entry 1NU2, were used to prepare the figure (*28*).

Isothermal Titration Calorimetry. All ITC measurements were carried out at 25 °C with the purified native or mutant Dab1 PTB domain protein at a concentration of 25−50 μM

in 20 mM PIPES buffer (pH 7.0) containing 150 mM NaCl and 0.2 mM DTT. A 14-residue synthetic peptide from the ApoER2 cytoplasmic tail (Invitrogen, acetyl-TKSMNFDN-PVYRKT-amide) was purified by reversed-phase HPLC and dissolved in the identical buffer for these titrations. The inositol headgroups of PI-4,5P_2 (Sigma, Echelon Biosciences), PI-1,4,5P_3 (Echelon Biosciences), and I4,5P_2 (Sigma) were dissolved in the identical buffer. To determine the phosphoinositide concentration, the hydrolyzed inorganic phosphate was quantified by the Ames method (*30*). The apparent substoichiometric concentration of PI-4,5P_2 required to saturate the Dab1 PTB domain in Figures 2B and 4B (calculated *n* values of 0.7 and 0.8, respectively) is attributed to inaccuracy in the measurement of the PI-4,5P_2 concentration, as the structure clearly indicates the presence of a single unique PI binding site. To perform the titrations, a stock solution of ligand was added in 7.5 μL increments to the solution containing the Dab1 PTB domain. To extract the dissociation constant, the enthalpy of binding, and the calculated entropy, data were plotted and analyzed with the Origin, version 5.0.

NMR Spectrometry. ^{15}N HSQC spectra of the Dab1 PTB domain with and without peptide and PI ligands were acquired on a Bruker 500 MHz spectrometer equipped with pulsed field gradient units and actively shielded Z-gradients. All spectra were acquired at 25 °C, using a triple-resonance cryoprobe and an ^{15}N HSQC pulse sequence with gradient water suppression. Data were processed with NmrPIPE (*31*) and analyzed using NmrView (*32*). ^{1}H chemical shifts were directly calibrated using ~0.3 mM 2,2-dimethyl-2-silapentane-5-sulfonate (DSS) as an internal standard. ^{15}N chemical shifts were referenced indirectly to DSS.

Titrations were performed on two identical 500 μL samples of ~350 μM ^{15}N-labeled protein in a 20 mM deuterated PIPES/10% D_2O mixture (pH 6.8) containing 150 mM NaCl. The first titration was carried out by successive additions of 5, 10, and 25 μL of a 10 mM PI-4,5P_2 (Sigma) stock solution in a 20 mM PIPES/10% D_2O mixture containing 150 mM NaCl, followed by 25, 25, and 40 μL additions of a 2.5 mM ApoER2 peptide stock in a 20 mM PIPES/10% D_2O mixture containing 150 mM NaCl. A second titration was carried out in the same way except that the order of peptide and PI-4,5P_2 addition was reversed.

RESULTS

Analysis of Native Disabled-1 PTB Domain and Ligand Interactions. The dissociation constant for binding of a 14-residue peptide from the ApoER2 tail to the Dab1 PTB domain is 3.0 ± 0.7 μM, consistent with previously published values for binding of ApoER2 and APP peptides under slightly different experimental conditions (Figure 2A; *28*, *33*). The binding constants of the Dab1 PTB domain for various PIs were also determined by ITC (Figure 2B−D). The binding affinity of the native PTB domain for PI-4,5P_2, the ligand used in the ternary complex crystals, is 1.2 μM (Figure 2B) under the same conditions.

It has been suggested that the Dab1 PTB domain shows some selectivity for binding to PI-4,5P_2 over other phosphoinositides (*33*). However, there appears to be no structural basis for selectivity between PI-4,5P_2 and PI-3,4,5P_3, as the preferred binding orientation of the PI-4,5P_2 ligand leaves the 3-phosphate position unobstructed (Figure 1). The structure thus suggests that the Dab1 PTB domain should be able to bind both PI-4,5P_2 and PI-3,4,5P_3 with similar affinities. To test whether Dab1 shows selectivity for PI-4,5P_2 over PI-3,4,5P_3, we also measured the dissociation constant for binding of PI-3,4,5P_3 by the Dab1 PTB domain. The measured dissociation constant of the PTB domain for PI-3,4,5P_3 is 2.0 μM, indicating that Dab1 displays little intrinsic selectivity for PI-4,5P_2 over PI-3,4,5P_3 (Figure 2C).

In the structure of the ternary complex, density for the PI-4,5P_2 ligand suggests that the bound PI-4,5P_2 can adopt either of two different orientations in the complex: one that places the 1-phosphate in the proximity of Arg76 of the Dab1 PTB domain and one in which the PI molecule has been rotated 180° and the 1-phosphate is no longer in the proximity of any PTB domain residue (*28*). Occupancy refinement of the Dab1 PTB domain ternary structure suggests a preference of approximately 3 to 1 for the first orientation over the second (*28*). To examine the influence of the 1-phosphate on binding affinity, we measured the dissociation constant of the Dab1 PTB domain for inositol 4,5-bisphosphate (I-4,5P_2), a molecule identical to the PI-4,5P_2 headgroup except that there is no phosphate at the 1-position. The dissociation constant for binding of I-4,5P_2 is 5.3 μM, approximately 5-fold lower than that for PI-4,5P_2 (Figure 2D), showing that only a minor increase in affinity results from inclusion of a phosphate group at the 1-position of the inositol ring. This finding is also consistent with the prior conclusion that the Dab1 PTB domain can bind PI-4,5P_2 in either orientation, with only a modest preference for the orientation with higher occupancy in our crystal structure (*28*).

Analysis of Disabled-1 PTB Domain Mutants. As the first step in assessing whether the two ligand-binding sites function independently, a series of PTB domain mutants were made where a single critical residue of either the PI binding site or the peptide binding site was mutated. The structural integrity of each of the mutant proteins was verified by a far-UV wavelength circular dichroism scan, which was compared to that of the native protein. The circular dichroism spectra of native Dab1 and the point mutants are virtually superimposable, indicating that none of the mutations dramatically alter the structure of the unliganded domain (Figure 3 and data not shown).

Binding of PI-4,5P_2 and of the 14-residue ApoER2 peptide was then assessed for each of these mutants by ITC (Table 1). For the PI binding site, three residues were targeted: Lys45, Lys82, and His81. Lysines 45 and 82 serve as bridging lysines that coordinate oxygens from both the 4- and 5-position phosphate groups of PI-4,5P_2 (Figure 1); mutation of these residues is predicted to dramatically reduce binding affinity. In contrast, Histidine 81 only contacts the 5-phosphate, and mutation of this residue is expected to have a less pronounced effect on binding affinity (Figure 1).

These predictions are indeed borne out in the affinity measurements, regardless of whether the residues are replaced with alanine or glutamate. Mutation of Lys45 or Lys82 to either alanine or glutamate abrogates detectable

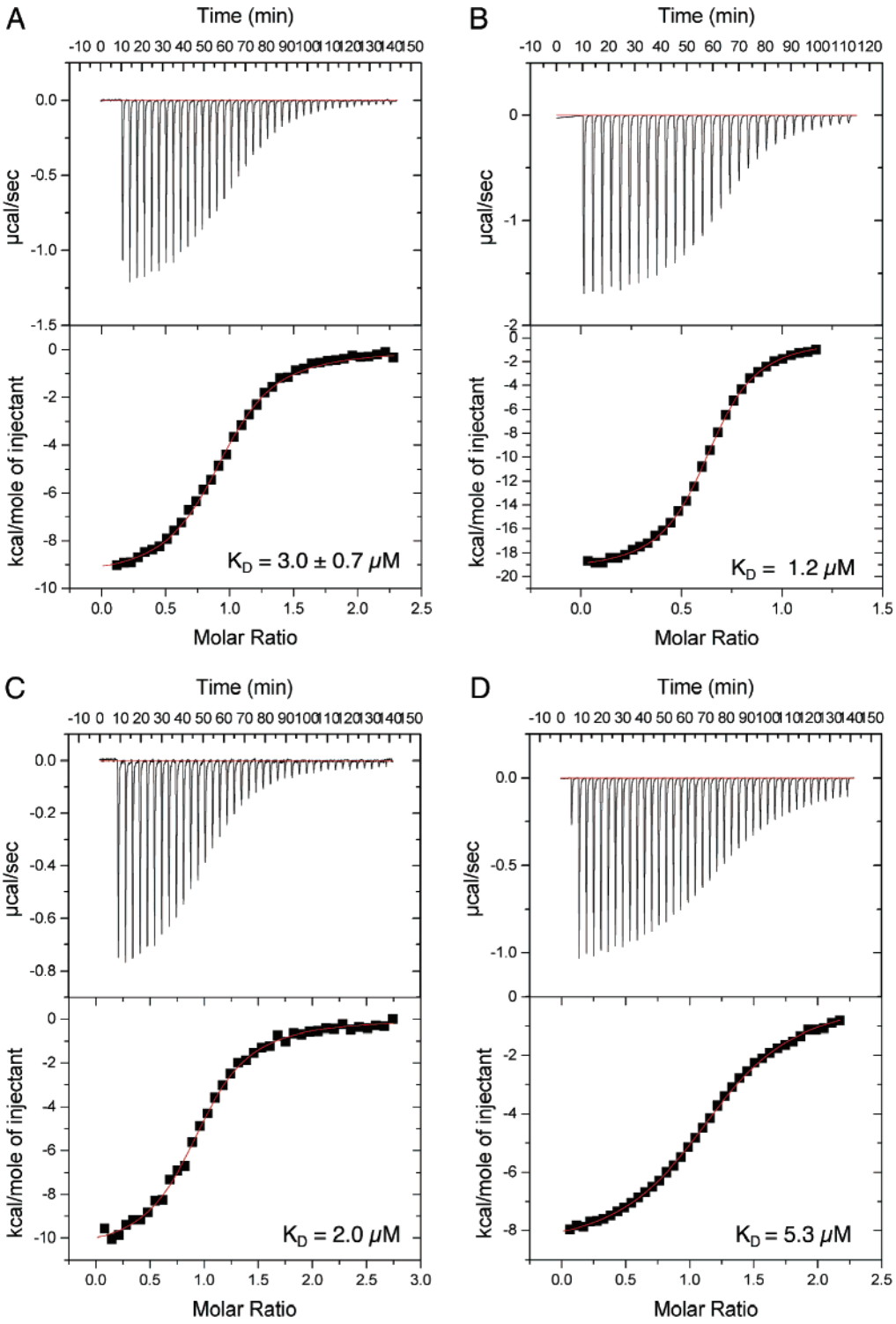

FIGURE 2: ITC measurements for binding of the wild-type Dab1 PTB domain to various ligands. All titrations were performed with 50 μM PTB domain, to which the ligand was added incrementally (see Experimental Procedures). To calculate the dissociation constant, data were fitted to a one-site binding model with Origin 5.0. (A) Binding of the PTB domain to the ApoER2 peptide. (B) Binding of the PTB domain to PI-4,5P_2. (C) Binding of the PTB domain to PI-3,4,5P_3. (D) Binding of the PTB domain to I-4,5P_2.

binding, and the His81 mutants exhibit K_D values from 20 to 100 times lower (Table 1).

All of the PI binding site mutants are still able to bind to the peptide with binding affinities comparable to that of the native PTB domain. The energetics involved in peptide binding also remain virtually unchanged; binding is still largely enthalpy driven, with enthalpy and entropy values in the same range as those seen for peptide binding by the native PTB domain (Table 1).

Similar findings hold for the peptide mutants. Two mutations were made: a previously characterized F158V mutation, which has been shown to lead to an approximately 20-fold decrease in peptide affinity (*33*), and an S114Y mutation. Serine 114 lies close to the binding pocket for the

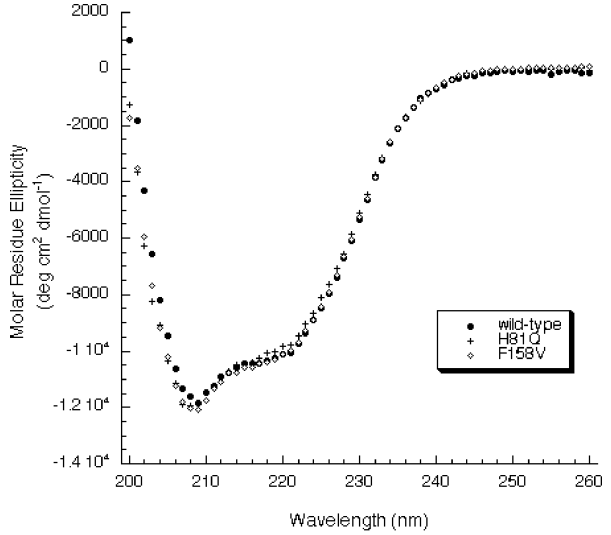

FIGURE 3: Far-UV CD spectra of Disabled-1 PTB domain mutants. Far-UV circular dichroism wavelength scans for the wild-type Disabled-1 PTB domain, the F158V peptide-binding mutant, and the H81Q PI-binding mutant.

Table 1: Dissociation Constants and Thermodynamics for Binding of Disabled-1 Mutants to the ApoER2 Peptide or PI-4,5P_2

protein	apo14 binding[a] (μM)	ΔH (kcal/mol)	$T\Delta S$ (kcal/mol)	PI-4,5P_2 binding[a] (μM)	ΔH (kcal/mol)	$T\Delta S$ (kcal/mol)
native	3.0 ± 0.7	−9.6	−1.9	1.2	−19.2	−11.1
H81A	3.2	−11.6	−0.4	24	−11.2	−4.6
H81Q	1.6	−10.8	−2.9	18	−9.8	−3.4
K45A	2.3	−10.1	−2.4	>50		
K45Q	2.9	−8.1	−0.6	>350		
K45E	2.2	−10.6	−2.9	>350		
K82A	1.4	−11.0	−3.0	~200		
K82Q	1.7	−14.5	−6.6	>350		
K45A/K82A	3.0	−8.8	−1.3	>350		
K45Q/K82Q	2.7	−9.3	−1.7	>350		
K45E/K82Q	2.1	−10.2	−2.5	>350		
S114Y	>175			1.2	−24.4	−16.3
F158V	28			0.6	−18.1	−9.6

[a] The estimated error in K_d upon repeated measurement is approximately ±25% (standard error of the mean), as assessed by repeated measurement of the K_d of the native Dab-1 PTB domain for the ApoER2 peptide.

peptide tyrosine, and replacement with a bulky aromatic residue should block peptide binding. Indeed, our ITC measurements show that the extent of peptide binding of the F158V mutant decreases by approximately 10-fold, while binding of the peptide to the S114Y mutant decreases by at least 70-fold; more accurate measurement of such weak binding is beyond the range of detection of the assay (Table 1). Nevertheless, both mutants bind PI-4,5P_2 with an affinity comparable to that of the native PTB domain, and the energetics remain the same as for the native protein (Table 1).

Independence of Ligand Binding As Measured by Calorimetry. To assess the effect of the presence of one ligand on binding to the other with the native PTB domain, affinity constants for the peptide and PI-4,5P_2 were measured again in the presence of saturating amounts of the other-site ligand. The presence of the second ligand has little effect on the binding constant for the first ligand, with a less than 2-fold change in the binding constant for either PI-4,5P_2 or peptide binding (Figure 4).

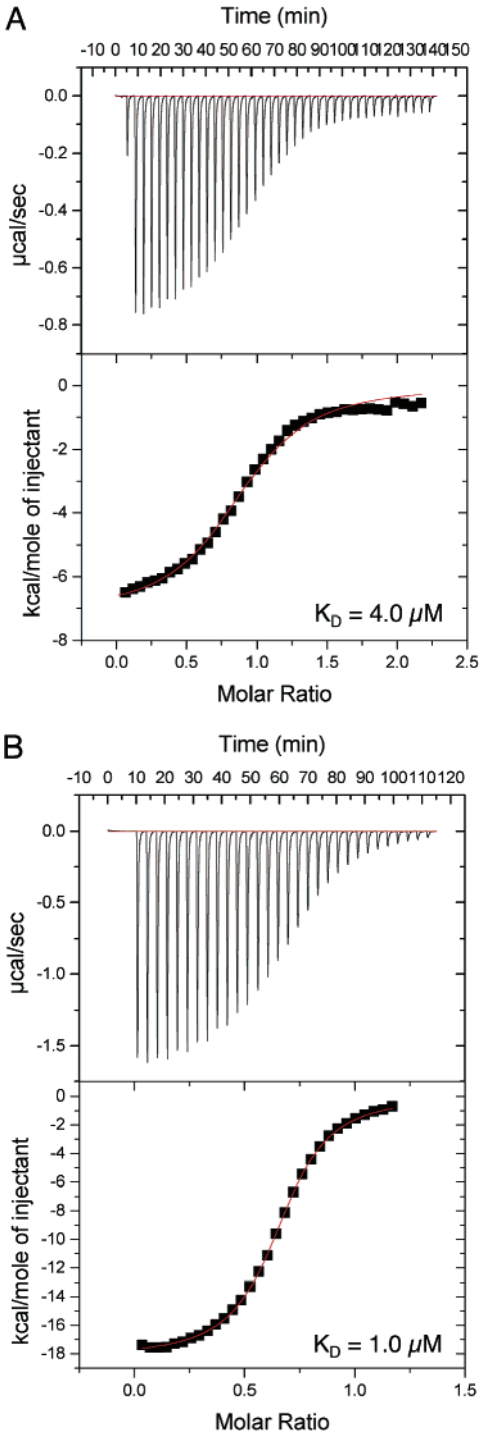

FIGURE 4: ITC measurements for binding of the native Dab1 PTB domain to one ligand in the presence of saturating concentrations of the second ligand. Measurements were performed as described in the legend of Figure 2. (A) Binding of the PTB domain to the ApoER2 peptide in the presence of a 2.5-fold molar excess of PI-4,5P_2 (present in excess of 100K_D). (B) Binding of the PTB domain to PI-4,5P_2 in the presence of a 2.5-fold molar excess of the ApoER2 peptide (present in excess of 50K_D).

NMR Titration Studies. To examine the structural perturbation of the backbone residues that takes place upon binding of peptide and PI ligands, the PTB domain of Dab1 was labeled with ^{15}N for use in solution NMR studies. $^1H-^{15}N$ HSQC spectra were recorded for a 350 μM sample of ^{15}N-labeled Dab1 PTB domain in 20 mM PIPES buffer (pH 6.8) containing 150 mM NaCl. The spectrum is well-dispersed,

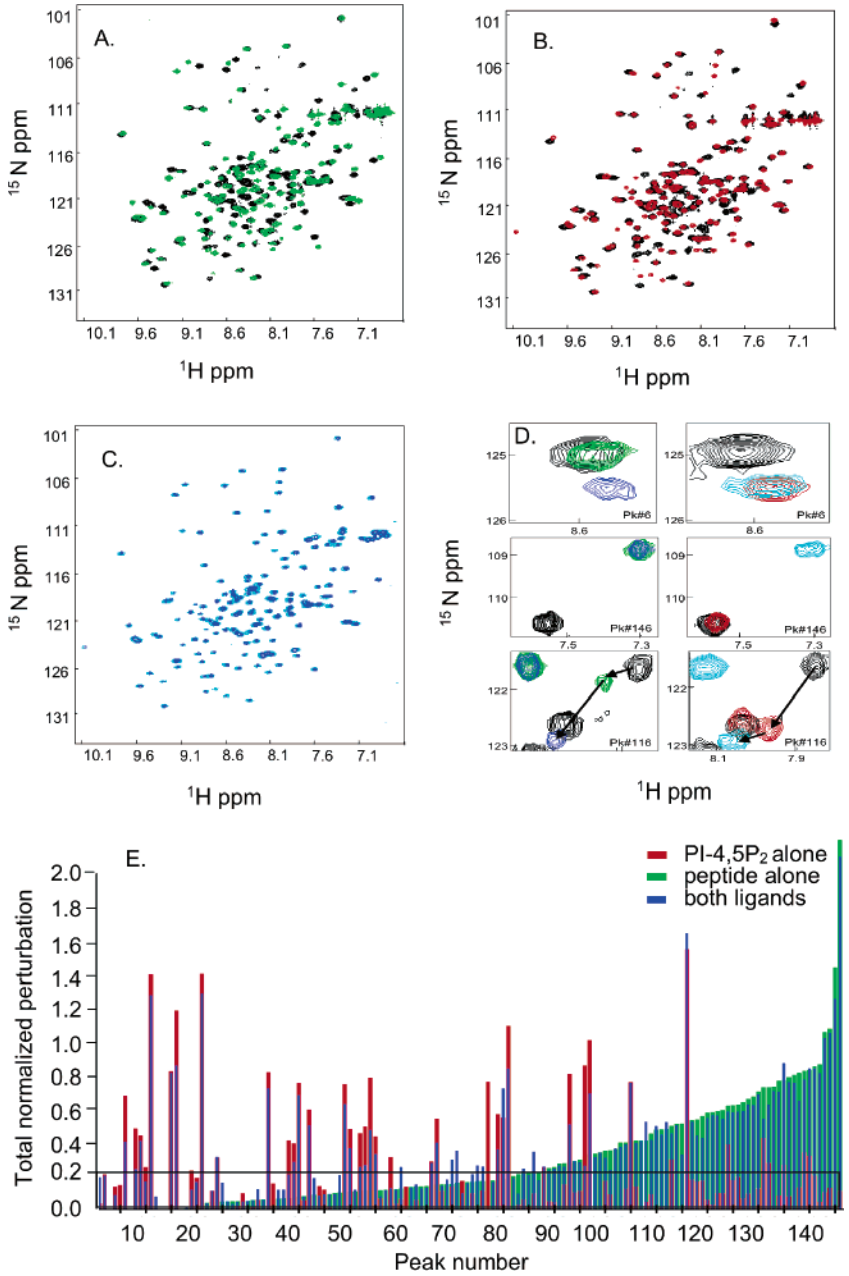

FIGURE 5: Effect of sequential ligand addition on the ^{1}H−^{15}N HSQC NMR spectrum of the Disabled-1 PTB domain. Increasing concentrations of the ligand were titrated into an ~350 μM sample of the ^{15}N-labeled Dab1 PTB domain. (A) Superposition of spectra acquired before and after saturation of the Dab1 PTB domain with the ApoER2 peptide: black for the Dab1 PTB domain alone and green for the Dab1 PTB domain after saturation with ApoER2 peptide. (B) Superposition of spectra acquired before and after saturation of the Dab1 PTB domain with PI-4,5P$_2$: black for the Dab1 PTB domain alone and red for the Dab1 PTB domain after saturation with PI-4,5P$_2$. (C) Overlay of spectra after addition of saturating amounts of both ligands: blue for addition of a saturating concentration of the ApoER2 peptide, followed by saturation with PI-4,5P$_2$, and cyan for addition of a saturating concentration of PI-4,5P$_2$, followed by saturation with the ApoER2 peptide. The order of ligand addition has no effect on the final positions of any peaks. (D) Effect of sequential addition of both ligands on the chemical shift of selected residues. Examples of peaks that move only in response to peptide binding (top panels), only in response to PI-4,5P$_2$ binding (middle panels), or in response to both peptide and PI-4,5P$_2$ binding (bottom panels). Left panels show data for addition of peptide, followed by addition of PI-4,5P$_2$. Right panels show data for addition of PI-4,5P$_2$, followed by addition of peptide. Peaks are colored as in panels A−C. (E) Plot of normalized chemical shift perturbation as a function of arbitrary peak number. For all of the 146 peaks resolved in the unliganded Dab1 HSQC spectrum, each peak was mapped to the closest peak in the spectrum after addition of peptide, PI-4,5P$_2$, or both ligands (green, red, and blue bars, respectively). The change in chemical shift induced upon binding of peptide, PI-4,5P$_2$, or both ligands was then calculated for each dimension (^{1}H and ^{15}N). The magnitude of the shift was then normalized to the maximum for each dimension, and the two values were added to obtain the total normalized perturbation. To create the final plot, peaks were sorted on the basis of the magnitude of the chemical shift change induced upon peptide binding. The threshold used to define perturbed residues, denoted by a black horizontal line, was set at a normalized value of 0.2.

and 146 backbone peaks could be readily distinguished. Increasing concentrations of either the peptide ligand or PI-4,5P$_2$ were then added, and the influence of the ligand on the spectrum was examined. Addition of the peptide ligand causes movement of 58 peaks (Figure 5A), while addition of PI-4,5P$_2$ moves a smaller set of 33 peaks (Figure 5B).

To determine whether the final structure of the ternary complex is independent of the order of addition of the two

ligands, the second ligand was then titrated into a sample already containing saturating amounts of the first ligand, and the effect on the spectrum was observed. The order of addition of the ligands has no effect on the final position of any peaks, and the final spectra are superimposable (Figure 5C). The vast majority of peaks arrive at their final positions after addition of either one ligand or the other, with only five peaks exhibiting significant perturbations from both ligands (Figure 5D,E).

DISCUSSION

Recently published crystal structures showing the Dab1 PTB domain bound to two ligands have allowed a more detailed analysis of how this remarkable dual-ligand binding domain functions. Our biophysical analysis of the Dab1 PTB domain shows that the binding of each of its two ligands is energetically independent of the other. Rather than using an allosteric mechanism, the Dab1 PTB domain appears to serve as a scaffold with two independent binding sites ready to accept either ligand without a preferred order of ligand binding.

The observed independence of the two binding sites is noteworthy when one considers that peptide binding to certain PTB domains seems to occur through an induced fit mechanism. A recent study investigating the coupling of folding and ligand binding in the Shc PTB domain shows that the peptide binding pocket of the Shc PTB domain is highly disordered in the absence of its peptide ligand (*34*). Upon peptide binding, the binding groove becomes fully constructed. The changes in $^{1}H-^{15}N$ HSQC chemical shifts observed upon addition of the peptide ligand to the Dab1 PTB domain suggest that, like Shc, this PTB domain also undergoes more significant rearrangements upon peptide binding, with movements occurring in more than 50 residues (Figure 5A). Since docking into the peptide binding groove requires contacts with several backbone amides and carbonyls, it is not surprising that binding of the peptide in the groove propagates beyond the binding site. The degree of induced fit upon peptide binding must vary among different PTB domains, as the IRS-1 and Dab2 PTB domains both crystallized in their apo forms; these structures show only small differences when compared to the liganded domains (*29*, *35*).

In contrast to peptide binding, PI binding is mediated through electrostatic side chain interactions, and thus, PI binding affects a much smaller number of residues within the Dab1 PTB domain. While peptide binding may be accompanied by locking of several strands of the β-sandwich, or clamping of the C-terminal α-helix, PI binding simply locks the side chain conformations of a group of solvent-exposed residues around the highly charged phosphate groups. It is clear that the PI binding patch is intact even in the unliganded Dab1 PTB domain, with any disorder centered primarily around the peptide binding groove, as order of ligand addition has no effect on either peptide or PI affinity for the PTB domain. Thus, the smaller, more segregated PI binding site is unaffected by local disorder elsewhere in the molecule, and both binding functions are preserved even when the protein's backbone structure is not completely locked in its peptide-bound conformation.

Although the phenomenon of intracellular dual-ligand binding domains such as the Dab1 PTB domain may be more widespread, structural data exist for only two additional intracellular domains thus far: the Pex13p SH3 domain (*36*) and the SAP SH2 domain (*37*). Pex13p is a membrane-bound protein that functions as a scaffold for the PTS1 receptor complex, and has been shown to bind to both the Pex5p and Pex14p proteins through its SH3 domain (*38*−*40*). Recent work by Wilmanns and colleagues has shown that while Pex14p exhibits canonical binding to the Pex13p SH3 domain, Pex5p binds to the opposite surface of the SH3 domain through an induced α-helical conformation. NMR titration analysis of the two binding sites in Pex13p also reveals that each site is able to bind ligand with a similar affinity whether the other ligand is present (*36*).

The SAP SH2 domain has also been shown to interact with two different proteins to form a ternary complex: the SH3 domain of Fyn kinase as well as the cytoplasmic tail of the SLAM receptor. The ternary structure shows a novel charged surface−surface interaction between the SAP SH2 domain and the Fyn SH3 domain that partially blocks the PxxP binding site on the Fyn SH3 domain, which may serve to prevent autoinhibition of Fyn (*37*). Since these two interactions involve independent surfaces on the SAP SH2 domain, it seems likely that these two sites also function independently, although the energetics of binding of the SAP SH2 domain to its two ligands has not been analyzed in detail.

In contrast to the site independence of the Dab1 PTB domain and the Pex13p SH3 domain, there is evidence that the PX domain of $p47^{phox}$ is able to bind to two lipid ligands and does so in an allosteric manner (*41*). SPR analysis of the binding of the $p47^{phox}$ domain to one of its two lipid ligands, PI-3,4P_2, indicates that binding is strengthened by 63-fold in the presence of the second lipid ligand, phosphatidic acid. Since these two lipid binding sites are thought to be adjacent, it is possible the proximity of the two sites necessitates such an allosteric effect. In the case of the Dab1 PTB domain and the Pex13p SH3 domain, the two binding sites are located on opposite faces of the domain, and therefore, any allosteric effect would have to be transmitted over a distance of 25−30 Å.

While the SAP SH2 domain, Pex13p SH3 domain, and Dab1 PTB domain all share the ability to bind to two ligands, the types of binding modes they use to do so differ. The SAP SH2 domain and Pex13p SH3 domain each have one canonical binding site as well as a second noncanonical binding site. In contrast, the Dab1 PTB domain exhibits two canonical binding sites: one peptide binding site that follows the conventional PTB domain binding mode and one PI binding site that is commonly seen in PH domains. In addition, close homologues of the Dab1 PTB domain present in the Dab2 and ARH proteins also bind both peptide and PI ligands (*22*, *23*, *42*, *43*). The Dab2 structure and an ARH homology model show an electrostatic charge distribution similar to that of Dab1, indicating PI binding most likely occurs at the same site in these PTB domains (*28*, *29*). Thus, while the SAP SH2 domain and Pex13p SH3 domain may be exceptional examples that have unique features leading to noncanonical binding of a second ligand, the Dab1 PTB domain is a prototype for a class of hybrid PTB−PH domains.

Similar biophysical studies of cytokine−receptor complexes, in which calorimetry has been used to examine site

independence, have shown that in some complexes the two binding sites function independently, such as in the LIF−LIF receptor−gp130 complex (*44*). In other cases, like the IL-6−IL-6 receptor−gp130 complex, the cytokine must first bind to its specific receptor before achieving a sufficiently high affinity to associate with gp130 (*45*).

Although our biophysical studies demonstrate energetic independence of the two ligand binding sites on the Dab1 PTB domain, there may well be functional synergy between peptide and PI binding *in vivo*. We postulate that PI binding by the Dab1 PTB domain may serve as a general mechanism for recruiting Dab1 to the plasma membrane rather than as a response to lipid second messengers produced by PI3 kinase. These studies, which show that the Dab1 PTB domain binds to phosphoinositide headgroups through an enthalpically driven mechanism with a K_D in the low micromolar range, and with little selectivity for PI-4,5P_2 versus PI-3,4,5P_3, are fully consistent with this proposal. In further support of this hypothesis, fractionation of primary neurons indicates that Dab1 is constitutively associated with the membrane (*46*). Thus, binding of PI-4,5P_2 by the PTB domain should increase the effective concentration of Dab1 at the membrane, placing it in the neighborhood of the ApoER2 C-terminal tail and facilitating association of the two proteins.

With the PTB domain mutants characterized here, it should now be possible to separate the biological roles of peptide and PI binding. Peptide binding mutants ought to be properly localized, but be inactive in signaling, whereas mutants that do not bind PI should neither be localized to the plasma membrane nor transduce signals if membrane recruitment is indeed required for signaling. Finally, if the only functional role for PI binding is to recruit Dab1 to the membrane, it may be possible functionally to replace the PI binding site on the Dab1 PTB domain with a myristoylation site or other localization sequence, thus underscoring the role of PI binding for proper localization. Study of our panel of Dab1 mutants, for example, in primary neurons or mouse models, should establish whether phosphoinositide binding by the PTB domain is required for Dab1 function *in vivo*, and these studies are in progress (P. C. Stolt, H. Bock, S. C. Blacklow, and J. Herz, unpublished work).

ACKNOWLEDGMENT

We thank Ju-fang Chang and Tom Ellenberger as well as Ann Georgi and Marc Kirschner for access to their ITC equipment as well as technical assistance.

REFERENCES

1. Pawson, T., and Nash, P. (2003) Assembly of cell regulatory systems through protein interaction domains, *Science 300*, 445−452.
2. Eck, M. J., Shoelson, S. E., and Harrison, S. (1993) Recognition of a high affinity phosphotyrosyl peptide by the Src homology 2 domain of p56^{lck}, *Nature 362*, 87−91.
3. Rickles, R. J., Botfield, M. C., Weng, Z., Taylor, J. A., Green, O. M., Brugge, J. S., and Zoller, M. J. (1994) Identification of Src, Fyn, Lyn, PI3K, and Abl SH3 domain ligands using phage display libraries, *EMBO J. 13*, 5598−5604.
4. Feng, S., Kasahara, C., Rickles, R. J., and Schreiber, S. L. (1995) Specific interactions outside the proline-rich core of two classes of Src homology 3 ligands, *Proc. Natl. Acad. Sci. U.S.A. 92*, 12408−12415.
5. Sparks, A. B., Rider, J. E., Hoffmann, N. G., Fowlkes, D. M., Quillam, L. A., and Kay, B. K. (1996) Distinct ligand preferences of Src homology 3 domains from Src, Yes, Abl, Cortactin, p53bb2, PLCgamma, Crk, and Grb2, *Proc. Natl. Acad. Sci. U.S.A. 93*, 1540−1544.
6. Lim, W. A., Richards, F. M., and Fox, R. O. (1994) Structural determinants of peptide-binding orientation and of sequence specificity in SH3 domains, *Nature 372*, 375−379.
7. Yu, H., Chen, J. K., Feng, S., Dalgarno, D. C., Brauer, A. W., and Schreiber, S. L. (1994) Structural basis for the binidng of proline-rich peptides to SH3 domains, *Cell 76*, 933−945.
8. Musacchio, A., Saraste, M., and Wilmanns, M. (1994) High-resolution crystal structures of tyrosine kinase SH3 domains complexed with proline-rich peptides, *Nat. Struct. Biol. 1*, 546−551.
9. Poy, F., Yaffe, M. B., Sayos, J., Saxena, K., Morra, M., Sumegi, J., Cantley, L. C., Terhorst, C., and Eck, M. J. (1999) Crystal Structures of the XLP Protein SAP Reveal a Class of SH2 Domains with Extended, Phosphotyrosine-Independent Sequence Recognition, *Mol. Cell 4*, 555−561.
10. Mongiovi, A. M., Romano, P. R., Panni, S., Mendoza, M., Wong, W. T., Musacchio, M., Cesareni, G., and Di Fiore, P. P. (1999) A novel peptide-SH3 interaction, *EMBO J. 18*, 5300−5309.
11. Berry, D. M., Nash, P., Liu, S. K., Pawson, T., and McGlade, C. J. (2002) A high-affinity Arg-X-X-Lys SH3 binding motif confers specificity for the interaction between Gads and SLP-76 in T cell signaling, *Curr. Biol. 12*, 1336−1341.
12. Lemmon, M. A., and Ferguson, K. M. (2000) Signal-dependent membrane targeting by pleckstrin homology (PH) domains, *Biochem. J. 350*, 1−18.
13. Blaikie, P., Immanuel, D., Wu, J., Li, N., Yajnik, V., and Margolis, B. (1994) A region in Shc distinct from the SH2 domain can bind tyrosine-phosphorylated growth factor receptors, *J. Biol. Chem. 269*, 32031−32034.
14. Kavanaugh, W. M., Turck, C. W., and Williams, L. T. (1995) PTB domain binding to signaling proteins through a sequence motif containing phosphotyrosine, *Science 268*, 1177−1179.
15. Kavanaugh, W. M., and Williams, L. T. (1994) An alternative to SH2 domains for binding tyrosine-phosphorylated proteins, *Science 266*, 1862−1865.
16. Howell, B. W., Lanier, L. M., Frank, R., Gertler, F. B., and Cooper, J. A. (1999) The disabled 1 phosphotyrosine-binding domain binds to the internalization signals of transmembrane glycoproteins and to phospholipids, *Mol. Cell Biol. 19*, 5179−5188.
17. Li, S. C., Zwahlen, C., Vincent, S. J., McGlade, C. J., Kay, L. E., Pawson, T., and Forman-Kay, J. D. (1998) Structure of a Numb PTB domain-peptide complex suggests a basis for diverse binding specificity, *Nat. Struct. Biol. 5*, 1075−1083.
18. Dhalluin, C., Yan, K., Plotnikova, O., Lee, K. W., Zeng, L., Kuti, M., Mujtaba, S., Goldfarb, M. P., and Zhou, M. M. (2000) Structural basis of SNT PTB domain interactions with distinct neurotrophic receptors, *Mol. Cell 6*, 921−929.
19. Zwahlen, C., Li, S. C., Kay, L. E., Pawson, T., and Forman-Kay, J. D. (2000) Multiple modes of peptide recognition by the PTB domain of the cell fate determinant Numb, *EMBO J. 19*, 1505−1515.
20. Zhou, M. M., Ravichandran, K. S., Olejniczak, E. F., Petros, A. M., Meadows, R. P., Sattler, M., Harlan, J. E., Wade, W. S., Burakoff, S. J., and Fesik, S. W. (1995) Structure and ligand recognition of the phosphotyrosine binding domain of Shc, *Nature 378*, 584−592.
21. Ravichandran, K. S., Zhou, M. M., Pratt, J. C., Harlan, J. E., Walk, S. F., Fesik, S. W., and Burakoff, S. J. (1997) Evidence for a requirement for both phospholipid and phosphotyrosine binding via the Shc phosphotyrosine-binding domain in vivo, *Mol. Cell Biol. 17*, 5540−5549.
22. Mishra, S. K., Keyel, P. A., Hawryluk, M. J., Agostinelli, N. R., Watkins, S. C., and Traub, L. M. (2002) Disabled-2 exhibits the properties of a cargo-selective endocytic clathrin adaptor, *EMBO J. 21*, 4915−4926.
23. Mishra, S. K., Watkins, S. C., and Traub, L. M. (2002) The autosomal recessive hypercholesterolemia (ARH) protein interfaces directly with the clathrin-coat machinery, *Proc. Natl. Acad. Sci. U.S.A. 99*, 16099−16104.
24. Rameh, L. E., Arvidsson, A., Carraway, K. L., III, Couvillon, A. D., Rathbun, G., Crompton, A., VanRenterghem, B., Czech, M. P., Ravichandran, K. S., Burakoff, S. J., Wang, D. S., Chen, C. S., and Cantley, L. C. (1997) A comparative analysis of the

phosphoinositide binding specificity of pleckstrin homology domains, *J. Biol. Chem. 272*, 22059−22066.
25. Howell, B. W., Hawkes, R., Soriano, P., and Cooper, J. A. (1997) Neuronal position in the developing brain is regulated by mouse disabled-1, *Nature 389*, 733−737.
26. Trommsdorff, M., Borg, J. P., Margolis, B., and Herz, J. (1998) Interaction of cytosolic adaptor proteins with neuronal apolipoprotein E receptors and the amyloid precursor protein, *J. Biol. Chem. 273*, 33556−33560.
27. Hiesberger, T., Trommsdorff, M., Howell, B. W., Goffinet, A., Mumby, M. C., Cooper, J. A., and Herz, J. (1999) Direct binding of Reelin to VLDL receptor and ApoE receptor 2 induces tyrosine phosphorylation of disabled-1 and modulates tau phosphorylation, *Neuron 24*, 481−489.
28. Stolt, P. C., Jeon, H., Song, H. K., Herz, J., Eck, M. J., and Blacklow, S. C. (2003) Origins of Peptide Selectivity and Phosphoinositide Binding Revealed by Crystal Structures of Disabled-1 Complexes, *Structure 11*, 569−579.
29. Yun, M., Keshvara, L., Park, C.-G., Zhang, Y.-M., Dickerson, J. B., Zheng, J., Rock, C. O., Curran, T., and Park, H.-W. (2003) Crystal Structures of the Dab Homology Domains of Mouse Disabled 1 and 2, *J. Biol. Chem. 278*, 36572−36581.
30. Ames, B. (1966) Assay of Inorganic Phosphate, Total Phosphate and Phosphatases, *Methods Enzymol. 8*, 115−118.
31. Delaglio, F., Grzesiek, G., Vuister, G., Pfeifer, J., and Bax, A. (1995) NMRPipe: a multidimensional spectral processing system based on UNIX pipes, *J. Biomol. NMR 6*, 227−293.
32. Johnson, B., and Blevins, R. (1994) NMRView: A computer program for the visualization and analysis of NMR data, *J. Biomol. NMR 4*, 603−614.
33. Howell, B. W., Herrick, T. M., and Cooper, J. A. (1999) Reelin-induced tryosine phosphorylation of disabled 1 during neuronal positioning, *Genes Dev. 13*, 643−648.
34. Farooq, A., Zeng, L., Yan, K. S., Ravichandran, K. S., and Zhou, M. M. (2003) Coupling of Folding and Binding in the PTB Domain of the Signaling Protein Shc, *Structure 11*, 905−913.
35. Eck, M. J., Dhe-Paganon, S., Trub, T., Nolte, R. T., and Shoelson, S. E. (1996) Structure of the IRS-1 PTB domain bound to the juxtamembrane region of the insulin receptor, *Cell 85*, 695−705.
36. Douangamath, A., Filipp, F. V., Klein, A. T. J., Barnett, P., Zou, P., Voorn-Brouwer, T., Vega, M. C., Mayans, O. M., Sattler, M., Distel, B., and Wilmanns, M. (2002) Topography for Independent Binding of α-Helical and PPII-Helical Ligands to a Peroxisomal SH3 Domain, *Mol. Cell 10*, 1007−1017.
37. Chan, B., Lanyi, A., Song, H. K., Griesbach, J., Simarro-Grande, M., Poy, F., Howie, D., Sumegi, J., Terhorst, C., and Eck, M. J. (2003) SAP couples Fyn to SLAM immune receptors, *Nat. Cell Biol. 5*, 155−160.
38. Bottger, G., Barnett, P., Klein, A. T., Kragt, A., Tabak, H. F., and Distel, B. (2000) The peroxisomal membrane protein Pex13p shows a novel mode of SH3 interaction, *EMBO J. 19*, 6382−6391.
39. Girzalsky, W., Rehling, P., Stein, K., Kipper, J., Blank, L., Kunau, W. H., and Erdmann, R. (1999) Involvement of Pex13p in Pex14p localization and peroxisomal targeting signal 2-dependent protein import into peroxisomes, *J. Cell Biol. 144*, 1151−1162.
40. Urquhart, A. J., Kennedy, D., Gould, S. J., and Crane, D. I. (2000) Interaction of Pex5p, the type 1 peroxisome targeting signal receptor, with the peroxisomal membrane proteins Pex14p and Pex13p, *J. Biol. Chem. 275*, 4127−4136.
41. Karathanassis, D., Stahelin, R. V., Bravo, J., Perisic, O., Pacold, C. M., Cho, W., and Williams, R. L. (2002) Binding of the PX domain of $p47^{phox}$ to phosphatidylinositol 3,4-bisphospate and phosphatidic acid is masked by an intramolecular interaction, *EMBO J. 21*, 5057−5068.
42. Morris, S. M., and Cooper, J. A. (2001) Disabled-2 colocalizes with the LDLR in clathrin-coated pits and interacts with AP-2, *Traffic 2*, 111−123.
43. He, G., Gupta, S., Michaely, P., Hobbs, H. H., and Cohen, J. C. (2002) ARH is a modular adaptor protein that interacts with the LDL receptor, clathirn, and AP-2, *J. Biol. Chem. 277*, 44044.
44. Boulanger, M. J., Bankovich, A. J., Kortemme, T., Baker, D., and Garcia, K. C. (2003) Convergent mechanisms for recognition of divergent cytokines by the shared signaling receptor gp130, *Mol. Cell 12*, 577−589.
45. Boulanger, M. J., Chow, D.-C., Brevnova, E. E., and Garcia, K. C. (2003) Hexameric structure and assembly of the Interleukin-6/IL-6 α-receptor/gp130 complex, *Science 300*, 2101−2104.
46. Bock, H. H., Jossin, Y., Liu, P., Forster, E., May, P., Goffinet, A., and Herz, J. (2003) Phosphatidylinositol 3-kinase interacts with the adaptor protein Dab1 in response to Reelin signaling and is required for normal cortical lamination, *J. Biol. Chem. 278*, 38772−38779.
47. Waksman, G., Shoelson, S. E., Pant, N., Cowburn, D., Kuriyan, J. (1993) Binding of a high affinity phosphotyrosyl peptide to the Src SH2 domain: Crystal structures of the complexed and peptide-free forms, *Cell 1993*, 779−790.

BI049092L